

Midazolam exhibits antitumour and anti-inflammatory effects in a mouse model of pancreatic ductal adenocarcinoma

日本大学大学院医学研究科博士課程

外科系麻酔科学専攻

大島雪乃

修了年 2023 年

指導教員 鈴木孝浩

Midazolam exhibits antitumour and anti-inflammatory effects in a mouse model of pancreatic ductal adenocarcinoma

Yukino Oshima¹, Makoto Sano^{2,*}, Ichie Kajiwara¹, Yoshimi Ichimaru³, Tomoaki Itaya¹, Tomoya Kuramochi¹, Emiko Hayashi⁴, Jinsuk Kim², Osamu Kitajima¹, Yohei Masugi⁵, Atsushi Masamune⁶, Hideaki Ijichi^{7,8}, Yukimoto Ishii² and Takahiro Suzuki¹

¹Department of Anesthesiology, Nihon University School of Medicine, Tokyo, Japan, ²Division of Medical Research Planning and Development, Nihon University School of Medicine, Tokyo, Japan, ³Faculty of Pharmaceutical Sciences, Shonan University of Medical Sciences, Yokohama, Japan, ⁴Department of Biochemistry and Molecular Biology, Nippon Medical School, Tokyo, Japan, ⁵Department of Pathology, Keio University School of Medicine, Tokyo, Japan, ⁶Division of Gastroenterology, Tohoku University Graduate School of Medicine, Sendai, Japan, ⁷Department of Gastroenterology, Graduate School of Medicine, The University of Tokyo, Tokyo, Japan and ⁸Clinical Nutrition Center, Graduate School of Medicine, The University of Tokyo, Tokyo, Japan

*Corresponding author. E-mail: sano.makoto@nihon-u.ac.jp

Abstract

Background: Anaesthesia and perioperative management contribute to long-term outcomes of patients with cancer, including pancreatic ductal adenocarcinoma. We assessed the antitumour, anti-inflammatory, and analgesic effects of midazolam on *LSL-Kras^{G12D/+};Trp53^{flox/flox};pdx-1^{cre/+}* transgenic mice with pancreatic ductal adenocarcinoma.

Methods: Six-week-old transgenic mice were administered midazolam 30 mg kg⁻¹ day⁻¹ p.o. (n=13); midazolam 30 mg kg⁻¹ day⁻¹ with 1-(2-chlorophenyl)-N-methyl-N(1-methylpropyl)-3-isoquinoline carboxamide (PK11195) 3 mg kg⁻¹ day⁻¹ i.p., a peripheral benzodiazepine receptor antagonist (n=10); or vehicle (water; n=14) until the humane endpoint. Cancer-associated pain was evaluated using hunching score and mouse grimace scale. Tumour stage and immuno-inflammatory status were determined histopathologically. Anti-proliferative and apoptotic potentials of midazolam were investigated using mouse pancreatic ductal adenocarcinoma cell lines.

Results: Midazolam significantly inhibited tumour size and proliferative index of Ki-67 and cyclins in pancreatic ductal adenocarcinoma, which was blocked by administration of PK11195. Local myeloperoxidase⁺ tumour-associated neutrophils, arginase-1⁺ M2-like tumour-associated macrophages, and CD11b⁺Ly-6G⁺ polymorphonuclear myeloid-derived suppressor cells were reduced by midazolam, which was antagonised by administration of PK11195. Hunching and mouse grimace scale were improved by midazolam, whereas the scores increased with midazolam+PK11195 treatment. Plasma pro-inflammatory cytokines, such as interleukin-6 and CC chemokine ligand (CCL)2, CCL3, and CCL5, were reduced by midazolam, whereas these cytokines increased with PK11195. Midazolam inhibited pancreatic ductal adenocarcinoma proliferation through downregulation of cyclins and cyclin-dependent kinases and induced apoptosis *in vitro*.

Conclusions: These results suggest that midazolam inhibits pancreatic ductal adenocarcinoma proliferation and local infiltration of tumour-associated neutrophils, tumour-associated macrophages, and polymorphonuclear myeloid-derived suppressor cells, thereby inhibiting pancreatic ductal adenocarcinoma progression.

Keywords: benzodiazepine receptor; GABA_A receptor; midazolam; pancreatic ductal adenocarcinoma; peripheral benzodiazepine receptor; translocator protein

Editor's key points

- Perioperative management has been implicated in the outcomes from cancer surgery.
- A mouse model of pancreatic ductal adenocarcinoma and tumour cell lines were used to investigate the antitumour, anti-inflammatory, and analgesic effects of midazolam.
- Midazolam suppressed proliferation of pancreatic ductal adenocarcinoma, cancer-associated fibroblasts and local infiltration of tumour-associated inflammatory cells, thereby inhibiting pancreatic ductal adenocarcinoma progression.
- These preclinical findings provide a basis for further study of the effects of midazolam and other perioperative drugs on long-term outcomes, such as recurrence and disease-free survival after cancer-related interventions.

Surgical resection of the primary tumour is generally the first treatment choice for patients with cancer, although recent studies have shown that perioperative management affects the long-term outcome of cancer patients.¹ Several reports have indicated that anaesthetics, including ketamine, propofol, and morphine, suppress the immune system.¹ Indeed, anaesthetics, such as dexmedetomidine, can enhance proliferative, invasive, and metastatic cancer activities.^{2,3} Therefore, it is important to select appropriate anaesthetic drugs for surgery in patients with cancer.

Midazolam (MDZ), a benzodiazepine anaesthetic, is widely used for induction of general anaesthesia, premedication, and procedural and postoperative sedation.^{4,5} The primary clinical effects of MDZ are mediated through central benzodiazepine receptors within neuronal γ -aminobutyric acid type A receptors, whereas MDZ has antitumour effects on lung cancer and glioma cells through peripheral benzodiazepine receptors (PBRs).² Overexpression of PBRs, renamed translocator protein (TSPO), is detected in various cancers, including pancreatic cancer.^{6,7} However, the effects of MDZ on pancreatic ductal adenocarcinoma (PDAC) remain unknown.

Pancreatic ductal adenocarcinoma has a high mortality rate compared with another malignant tumours.⁸ The frequency of surgical resection in patients with pancreatic cancer is increasing because of developing preoperative neoadjuvant chemotherapy. Patients with resectable PDAC who are undergoing surgery need anaesthetics for preoperative and postoperative management, whilst patients with unresectable PDAC also need appropriate care, including inhibition of cancer-associated pain. Midazolam inhibits macrophage and neutrophilic functions in non-cancer pathogenesis.⁹ Infiltration of pro-inflammatory M2 tumour-associated macrophages (TAMs) and tumour-associated neutrophils (TANs) is associated with cancer progression^{10,11} and cancer-associated inflammatory pain.¹² We hypothesised that MDZ has antitumour, anti-inflammatory, and analgesic effects in a mouse model of PDAC.

We used a transgenic PDAC mouse model (LSL-Kras^{G12D/+}; Trp53^{flox/flox}; Pdx-1^{cre/+} [KPPC])¹³ to evaluate the effects of MDZ on

PDAC, tumour-associated inflammatory cells, and cancer-associated pain.

Methods

Reagents

Midazolam (Maruishi Pharmaceutical Co., Ltd, Osaka, Japan; Sandoz, Tokyo, Japan) and 1-(2-chlorophenyl)-N-methyl-N(1-methylpropyl)-3-isoquinoline carboxamide (PK11195; Abcam Japan, Tokyo, Japan) were diluted with distilled water or dimethyl sulphoxide (DMSO), respectively.

Cell lines

Murine PDAC cell lines (#146, 147, and 244) were previously established from LSL-Kras^{G12D/+}; Trp53^{flox/+}; Pdx-1^{cre/+} (KPC^{flox}) mice.¹⁴ Human pancreatic stellate cell (hPSC) lines (1, 5, and 14) were obtained from RIKEN BioResource Research Center Cell Bank (Tsukuba, Ibaraki, Japan).¹³

Proliferation assay

Using an alamarBlue[®] proliferation assay (Thermo Fisher Scientific, Waltham, MA, USA), cells (1×10^4) were cultured in 96-well plates and treated with MDZ 1, 3, 10, 30, 100, or 300 μ M for 24 h. Experiments were performed in triplicate and repeated at least twice, as described.¹⁵

Cell-cycle analysis

Cells were treated with MDZ 40 or 400 μ M for 24 h. After staining with propidium iodide, cells were measured by flow cytometer, and cell-cycle analysis was performed by FlowJo software version 10 (Becton, Dickinson and Company, Franklin Lakes, NJ, USA).

Immunoblotting of cell-cycle-associated molecules

Cells were cultured for 24 h in the presence of MDZ, PK11195, or vehicle control (water or DMSO). The detailed protocol for immunoblotting has been reported.¹⁵

Detection of apoptosis by annexin V–propidium iodide double-staining analysis

Apoptotic cells were detected with Alexa Fluor[®] 488 annexin V/dead cell apoptosis kit (Life Technologies, Invitrogen, Carlsbad, CA, USA), as described.¹⁵

Administration of midazolam and PK11195

LSL-Kras^{G12D/+}; Trp53^{flox/flox}; Pdx-1^{cre/+} mice, which is a spontaneous PDAC mouse model under innate immunoinflammatory conditions,¹³ were separated into three groups. Six-week-old KPPC mice were administered MDZ 30 mg kg⁻¹ day⁻¹ p.o. (producing neither sedation nor hypoxaemia; $n=13$) or water vehicle ($n=14$) every day until the humane endpoint (when mice showed no activity, including grooming, food intake of <1 g day⁻¹, or $>20\%$ body weight loss over several days). Another group of 6-week-old KPPC mice was injected i.p. with PK11195 3 mg kg⁻¹ day⁻¹, a TSPO ligand, six times per week with MDZ 30 mg kg⁻¹ day⁻¹ p.o. ($n=10$) until the humane

endpoint. Cre-negative control mice were obtained from the same littermates. Data from vehicle-treated KPPC and normal control mice¹³ were used to reduce experimental animal use according to Animal Research: Reporting of In Vivo Experiments (ARRIVE) guidelines.

All animals were kept in pathogen-free housing with abundant food and water and killed by carbon dioxide at the humane endpoint under ARRIVE and institutional guidelines approved by the Nihon University School of Medicine Animal Care and Use Committee (AP18MED074 and AP19MED034).

Pain analysis

Two blinded investigators assessed cancer-associated pain using the hunching score, including exploratory behaviour (score of 0–4) and the mouse grimace scale (MGS) (score of 0–2 each; total score of 10), as reported.¹³

Autopsy

Autopsy was performed at the study endpoint. Total pancreatic weight was measured, and the tumour volumes were calculated as width × length × height. All samples were weighed and fixed in neutral buffered formalin 10%.

Immunohistochemistry

Immunostaining of pancreatic tumours, except for dead animals and tumours with ischaemic and massive central necrosis, was performed, as described.¹⁶ Cases with unclear staining of each internal control were excluded. We counted the number of positive cells in at least three fields (200×) in a representative specimen.

Cytokine antibody array of plasma

Murine plasma samples were obtained from the heart of control mice and KPPC mice groups at the study endpoint. We analysed cytokine concentrations of pooled plasma ($n=4$ each), except for icteric and haemolytic samples, using a RayBio® C-Series Mouse Cytokine Antibody Array 1000 (RayBiotech, Inc., Norcross, GA, USA) according to the manufacturer's instructions.¹⁷

Statistical analysis

For comparison of survival using Kaplan–Meier analyses, we used the log-rank test for univariate survival analyses. Tumour volumes and histopathological analyses were performed using parametric Tukey–Kramer test or non-parametric Steel–Dwass test with EZR (Easy R) software version 1.54.¹⁸ The significance of the differences in cumulative cancer pain was analysed by *post hoc* Tukey test after one-way analysis of variance using SPSS software version 25.0 (IBM Corp., Armonk, NY, USA). $P<0.05$ was considered statistically significant.

Results

Midazolam inhibited tumour proliferation by downregulation of cyclins *in vivo*

To determine the effects of MDZ on a pancreatic cancer *in vivo*, 6-week-old KPPC mice were treated with MDZ, MDZ and PK11195 (MDZ+PK11195), or water vehicle (Fig. 1a). Solid

pancreatic tumour nodules were detected in the three KPPC groups (Fig. 1b). Tumour size and frequency of direct invasion of peripheral tissue/organ, but not distant metastasis, were lower with administration of MDZ compared with vehicle-treated mice, and MDZ-induced tumour size reduction was reversed by treatment with PK11195 (Fig. 1c; Supplementary Tables 1–3). The proliferative Ki-67 labelling index of epithelial K-19⁺ PDAC component in KPPC mice was significantly reduced by MDZ (16.5%) compared with vehicle-treated KPPC mice (30.5%; Fig. 1d and e). In contrast, the reduced Ki-67 labelling index in PDAC was significantly elevated by treatment with MDZ+PK11195 (32.5%) compared with treatment with MDZ alone. Cyclins D1, A2, and B1 decreased in the PDAC component by administration of MDZ, whereas the inhibitory effects of MDZ were antagonised by treatment with PK11195 (Fig. 1d and e). No significant difference in survival was observed amongst the three groups of KPPC mice treated with MDZ (mean survival time 63.5 days), MDZ+PK11195 (62.7 days), or vehicle (61.1 days; Supplementary Fig. 1).

Midazolam inhibited local infiltration of inflammatory cells

We determined the effects of MDZ on the immunoinflammatory micro-environment of PDAC. Local infiltration of myeloperoxidase⁺ (MPO⁺) TANs, which are associated with cancer progression,¹⁰ was reduced in MDZ-treated KPPC mice (Fig. 2a and b). In contrast, MPO⁺ TANs were increased with MDZ+PK11195 compared with MDZ alone. There was no significant difference in inducible nitric oxide synthase⁺ antitumour M1-like TAMs¹⁰ amongst the three groups. Meanwhile, arginase-1⁺ pro-inflammatory M2-like TAMs¹⁰ were reduced by administration of MDZ and MDZ+PK11195. No significant difference in cytotoxic CD8⁺ T cells was observed between groups.

We studied local myeloid-derived suppressor cells because they enhance PDAC progression and are correlated with a poor prognosis clinically.¹⁹ Midazolam inhibited local infiltration of CD11b⁺Ly-6G⁺ polymorphonuclear myeloid-derived suppressor cells (PMN-MDSCs) in KPPC mice (Fig. 2c and d), whereas PMN-MDSCs were increased by MDZ+PK11195. Similar to the results in pancreatic tumours, MPO⁺ granulocytic lineages in bone marrow were reduced by MDZ, and this reduction was antagonised by MDZ+PK11195 (Supplementary Fig. 2).

We investigated MDZ effects on desmoplastic reactions with proliferation of cancer-associated fibroblasts (CAFs) and tumour angiogenesis. Masson's trichrome stain indicated that blue thickened collagen fibres surrounded the PDAC in vehicle-treated KPPC mice (Fig. 3a), whereas thin fibres were observed around PDAC nests in the mice administered MDZ and MDZ+PK11195. Similar to the results of Masson's trichrome staining, α -smooth muscle actin (α -SMA)⁺ CAFs¹⁶ were significantly reduced by treatment with MDZ or MDZ+PK11195 compared with vehicle-treated mice (Fig. 3a and b). We observed no difference in the number of CD31⁺ tumour blood vessels between the three groups. However, CD31⁺ micro-vessel density increased in mice treated with MDZ+PK11195.

Midazolam reduced pain signs and inflammatory cytokines in KPPC mice

We investigated the effect of MDZ on cancer-associated pain in KPPC mice, which demonstrate signs of pain, including a severe rounded-back posture (Fig. 4a).¹³ Midazolam-treated

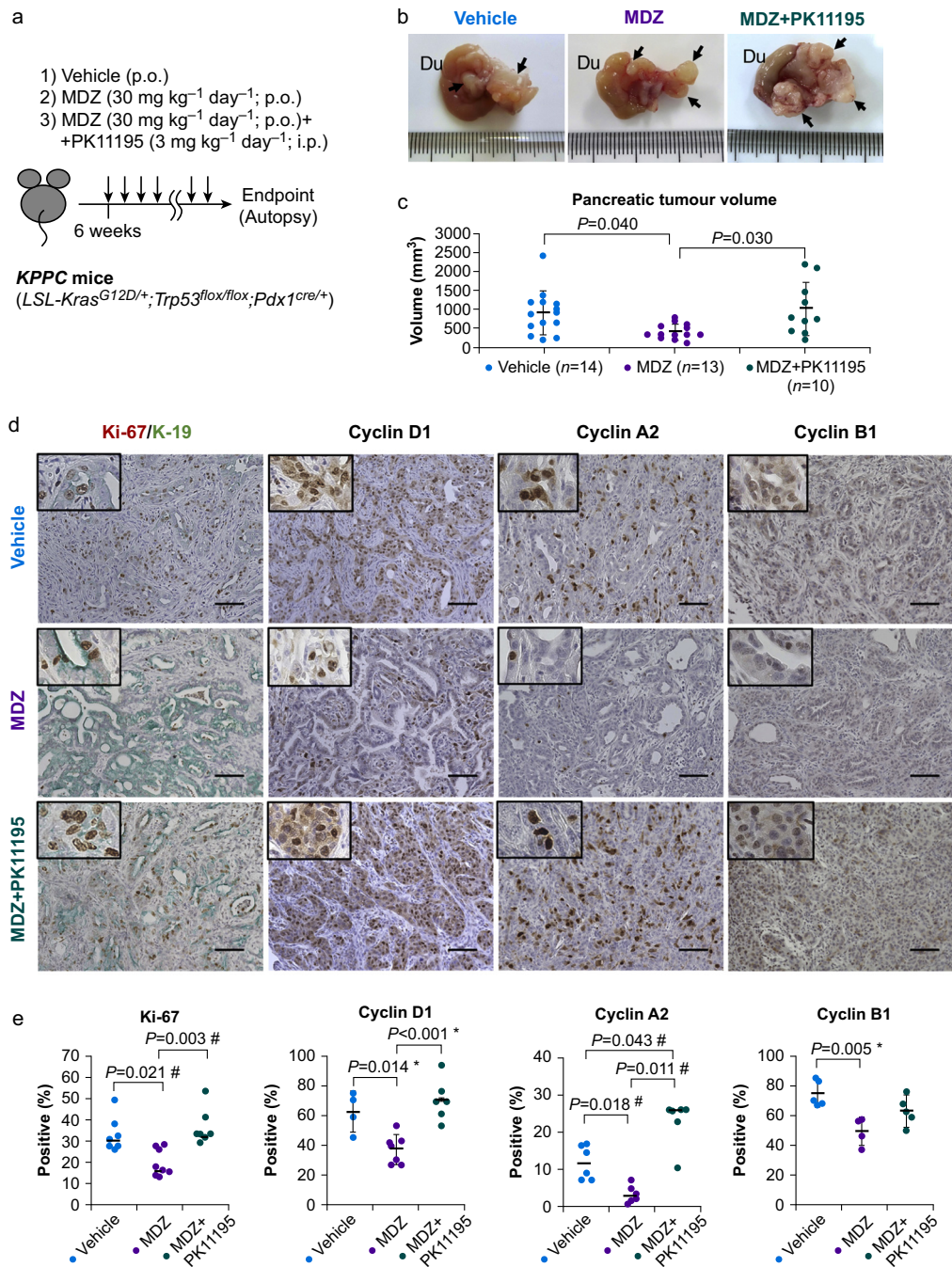


Fig 1. Inhibition of pancreatic ductal adenocarcinoma proliferation by MDZ in the mouse model *LSL-Kras^{G12D/+}; Trp53^{fllox/fllox}; Pdx-1^{cre/+}* (KPPC). (a) Experimental design. (b) Gross appearance (arrows, tumour nodules; Du, duodenum) and (c) volume of pancreatic tumour in KPPC mice with administration of MDZ (n=13), MDZ+PK11195 (n=10), or vehicle water (n=14). Data are presented as mean (SD). P=0.040, MDZ (n=13) vs vehicle (n=14); P=0.030, MDZ (n=13) vs MDZ+PK11195 (n=10); P=0.977, MDZ+PK11195 (n=10) vs vehicle (n=14) by non-parametric Steel–Dwass test. (d) Histopathological features, including staining for Ki-67 in K-19⁺ PDAC cells and cyclins D1, A2, and B1 (200×). Insets, 400× original magnification. Scale bars, 100 μm. (e) Quantification of the staining in (d). Data are presented as mean (SD) (normality data) or median values (non-normality data). Ki-67; P=0.021, MDZ (n=8) vs vehicle (n=7); P=0.003, MDZ (n=8) vs MDZ+PK11195 (n=7); P=0.372, MDZ+PK11195 (n=7) vs vehicle (n=7) by Steel–Dwass test (#). Cyclin D1; P=0.014, 95% CI [5.1; 45.0], MDZ (n=7) vs vehicle (n=4); P<0.001, 95% CI [15.4; 50.8], MDZ (n=7) vs MDZ+PK11195 (n=6); P=0.572, 95% CI [-28.6; 12.5], MDZ+PK11195 (n=6) vs vehicle (n=4) by parametric Tukey–Kramer test (*). Cyclin A2; P=0.018, MDZ (n=6) vs vehicle (n=6); P=0.011, MDZ (n=6) vs MDZ+PK11195 (n=6); P=0.043, MDZ+PK11195 (n=6) vs vehicle (n=6) by Steel–Dwass test (#). Cyclin B1; P=0.005, 95% CI [8.2; 41.6], MDZ (n=4) vs vehicle (n=5); P=0.118, 95% CI [-3.2; 30.1], MDZ (n=4) vs MDZ+PK11195 (n=5); P=0.166, 95% CI [-4.3; 27.2], MDZ+PK11195 (n=5) vs vehicle (n=5) by Tukey–Kramer test (*). CI, confidence interval; iNOS, inducible nitric oxide synthase; MDZ, midazolam; MPO, myeloperoxidase; PDAC, pancreatic ductal adenocarcinoma; PK11195, 1-(2-chlorophenyl)-N-methyl-N(1-methylpropyl)-3-isoquinoline carboxamide; SD, standard deviation.

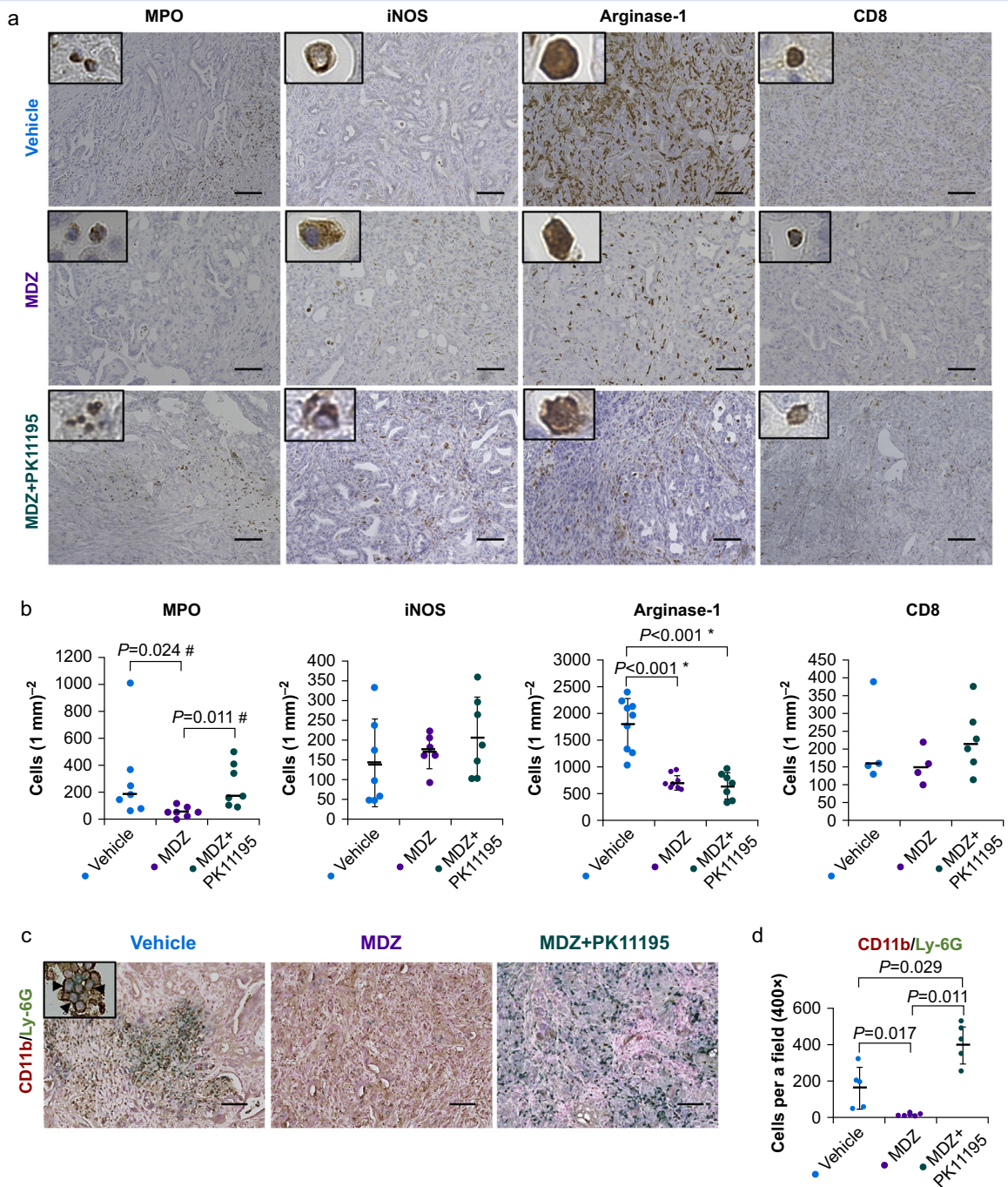


Fig 2. Inhibition of inflammatory cell infiltration by midazolam in KPPC mice. (a) MPO⁺ TANs and arginase1⁺ M2-like TAMs, but not iNOS⁺ M1-like TAMs and CD8⁺ cytotoxic T cells, were reduced with administration of MDZ (200 \times). Insets, 400 \times original magnification. (b) Quantification of the staining in (a). Data are presented as mean (standard deviation [sd]) or median values. MPO, $P=0.024$, MDZ ($n=7$) vs vehicle ($n=7$); $P=0.011$, MDZ ($n=7$) vs MDZ+PK11195 ($n=7$); $P=0.945$, MDZ+PK11195 ($n=7$) vs vehicle ($n=7$) by Steel–Dwass test (#). iNOS; $P=0.754$, MDZ ($n=6$) vs vehicle ($n=7$); $P=0.903$, MDZ ($n=6$) vs MDZ+PK11195 ($n=7$); $P=0.305$, MDZ+PK11195 ($n=7$) vs vehicle ($n=7$) by Steel–Dwass test. Arginase-1; $P<0.001$, 95% CI [687; 1509], MDZ ($n=8$) vs vehicle ($n=9$); $P=0.944$, 95% CI [-494; 381], MDZ ($n=8$) vs MDZ+PK11195 ($n=7$); $P<0.001$, 95% CI [728; 1580], MDZ+PK11195 ($n=7$) vs vehicle ($n=9$) by Tukey–Kramer test (*). CD8; $P=0.832$, MDZ ($n=4$) vs vehicle ($n=4$); $P=0.295$, MDZ ($n=4$) vs MDZ+PK11195 ($n=6$); $P=0.798$, MDZ+PK11195 ($n=6$) vs vehicle ($n=4$) by Steel–Dwass test. (c) PMN-MDSCs were detected by double staining for CD11b (brown) and Ly-6G (green) (200 \times). Insets, 400 \times original magnification (arrowheads, CD11b⁺Ly-6G⁺ PMN-MDSCs). (d) Quantification of the staining in (c). Scale bars, 100 μ m. Data are presented as mean (SD). $P=0.017$, MDZ ($n=5$) vs vehicle ($n=5$); $P=0.011$, MDZ ($n=5$) vs MDZ+PK11195 ($n=5$); $P=0.029$, MDZ+PK11195 ($n=5$) vs vehicle ($n=5$) by Steel–Dwass test. CI, confidence interval; iNOS, inducible nitric oxide synthase; MDZ, midazolam; MPO, myeloperoxidase; PDAC, pancreatic ductal adenocarcinoma; PK11195, 1-(2-chlorophenyl)-N-methyl-N(1-methylpropyl)-3-isoquinoline carboxamide; PMN-MDSC, polymorphonuclear myeloid-derived suppressor cell; TAM, tumour-associated macrophage; TAN, tumour-associated neutrophil.

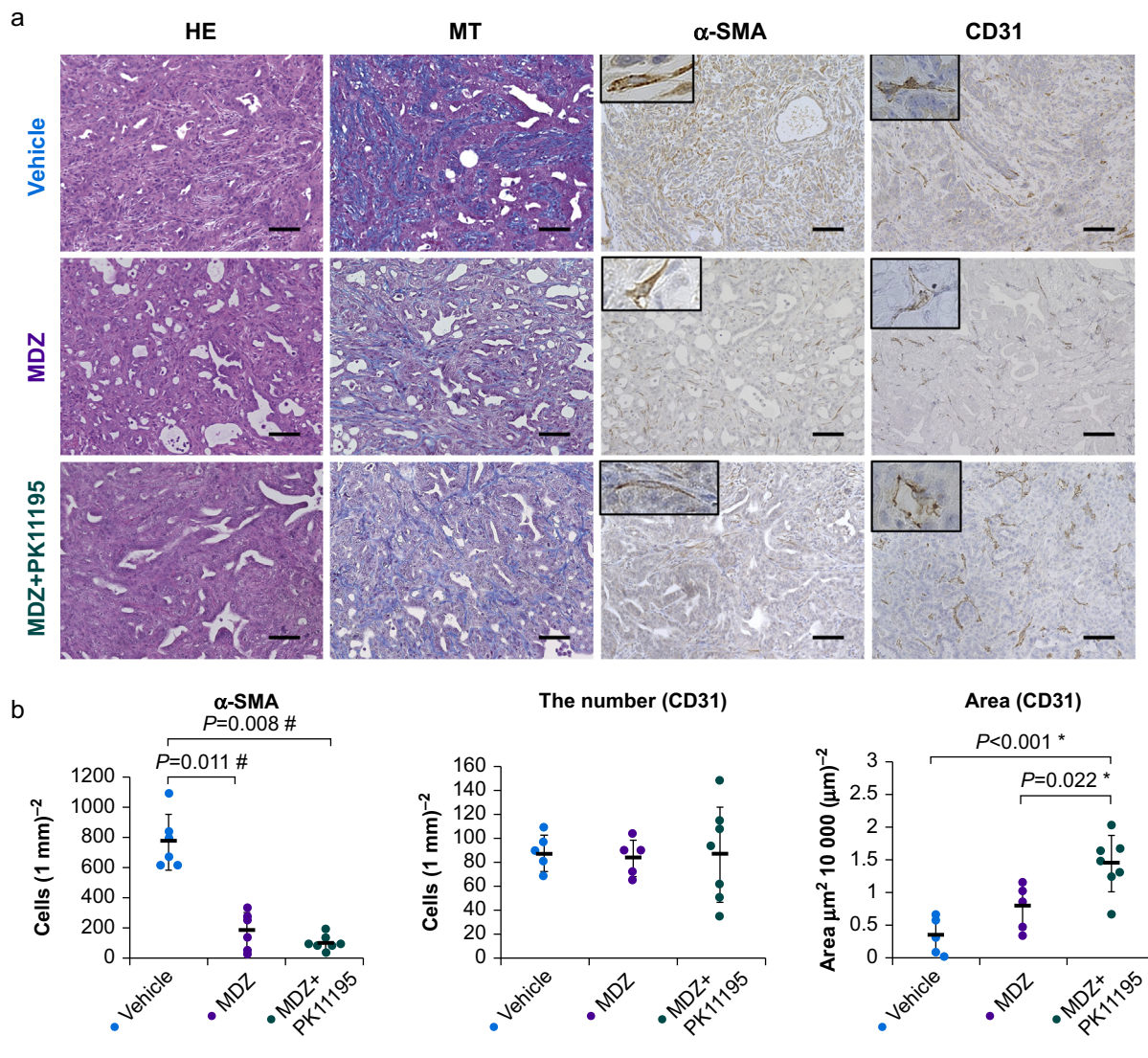


Fig 3. Reduction of α -SMA⁺ cancer-associated fibroblasts by administration of midazolam. (a) α -SMA⁺ cancer-associated fibroblasts and CD31⁺ tumour vessels in mice treated with MDZ and MDZ+PK11195. Insets, 400 \times original magnification. Scale bars, 100 μ m. (b) Quantification of the staining in (a). Data are presented as mean (standard deviation). α -SMA; $P=0.011$, MDZ ($n=6$) vs vehicle ($n=6$); $P=0.667$, MDZ ($n=6$) vs MDZ+PK11195 ($n=7$); $P=0.008$, MDZ+PK11195 ($n=7$) vs vehicle ($n=6$) by non-parametric Steel–Dwass test (#). The number of CD31; $P=0.970$, 95% CI [−42.7; 51.0], MDZ ($n=5$) vs vehicle ($n=5$); $P=0.977$, 95% CI [−40.0; 46.8], MDZ ($n=5$) vs MDZ+PK11195 ($n=7$); $P=0.999$, 95% CI [−42.6; 44.1], MDZ+PK11195 ($n=7$) vs vehicle ($n=5$) by Tukey–Kramer test. Area of CD31; $P=0.182$, 95% CI [−1.06; 0.17], MDZ ($n=5$) vs vehicle ($n=5$); $P=0.022$, 95% CI [0.09; 1.23], MDZ ($n=5$) vs MDZ+PK11195 ($n=7$); $P<0.001$, 95% CI [−1.67; −0.53], MDZ+PK11195 ($n=7$) vs vehicle ($n=5$) by Tukey–Kramer test (*). CI, confidence interval; MDZ, midazolam; PK11195, 1-(2-chlorophenyl)-N-methyl-N(1-methylpropyl)-3-isouquinoline carboxamide; α -SMA, α -smooth muscle actin.

KPPC mice showed a mild rounded-back posture, whereas the rounded-back posture progressed with MDZ+PK11195. The hunching scores decreased significantly with MDZ treatment during 0–26 premortal days (pmd) compared with vehicle-treated mice (Fig. 4b; Supplementary Fig. 2). Likewise, MGS scores were improved during 0–21 pmd in MDZ-treated KPPC mice compared with vehicle-treated mice (Fig. 4c; Supplementary Fig. 3). The effects of MDZ on hunching and MGS scores were reversed with MDZ+PK11195. In control mice, the hunching and MGS scores remained low during the observation period (Supplementary Fig. 4).

To elucidate the mechanism of pain relief by MDZ in the KPPC model, we investigated plasma cytokine concentrations (Fig. 4d; Supplementary Figs. 5–14). Cytokine antibody array using pooled plasma revealed that the major pain-associated cytokines tumour necrosis factor (TNF)- α , interleukin (IL)-6, and IL-1 α ¹³ increased in KPPC mice compared with control mice (Fig. 4d). These cytokines decreased in MDZ-treated mice, whereas IL-1 α and IL-6 increased in mice administered MDZ+PK11195 compared with MDZ-treated mice. We analysed the plasma concentrations of TAN- and MDSC-related cytokines. MDZ, but not MDZ+PK11195, reduced local infiltration of

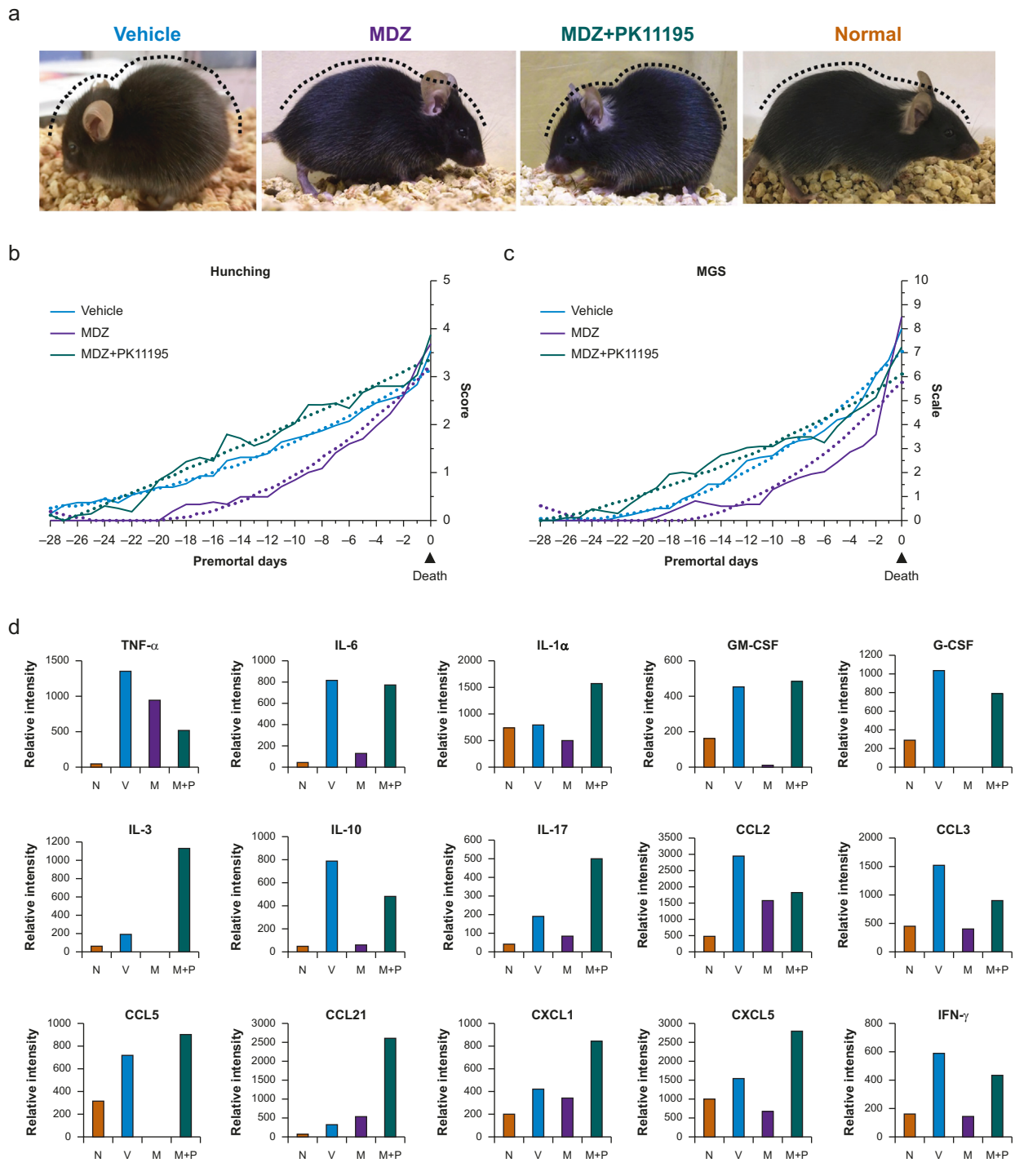


Fig 4. Modulation of inflammatory cytokines and cancer-associated pain by midazolam. (a) Representative vehicle-treated KPPC mouse showing signs of pain, including severe rounded-back posture (hunching score 4) and moderate nose-and-cheek bulge (MGS 10). MDZ-treated KPPC mouse (hunching score 3 and MGS 6). KPPC mouse treated with MDZ+PK11195 (hunching score 4 and MGS 8). No sign of pain in normal control mouse. (b) Mean scores of hunching and (c) MGS in KPPC mice treated with MDZ ($n=11$), MDZ+PK11195 ($n=10$), and vehicle water ($n=11$). (d) Pooled plasma concentrations ($n=4$ each) of cytokines in normal control (N) and KPPC mice with administration of MDZ (M), MDZ+PK11195 (M+P), or water vehicle (V). Data are presented as mean of two array spots. CCL, CC chemokine ligand; CXCL, C-X-C motif ligand; G-CSF, granulocyte-colony stimulating factor; GM-CSF, granulocyte macrophage colony-stimulating factor; IFN- γ , interferon- γ ; IL, interleukin; MDZ, midazolam; MGS, mouse grimace scale; PK11195, 1-(2-chlorophenyl)-N-methyl-N(1-methylpropyl)-3-isoquinoline carboxamide; TNF, tumour necrosis factor.

TANs and PMN-MDSCs. Granulocyte colony-stimulating factor (G-CSF), granulocyte macrophage colony-stimulating factor (GM-CSF), IL-3, and IL-6, which are closely related to granulocyte differentiation in bone marrow, were reduced by treatment with MDZ, which was antagonised by treatment with MDZ+PK11195. Midazolam also reduced TNF- α , IL-17, C-X-C motif ligand (CXCL)1, CXCL5, and interferon- γ , which enhance TAN recruitment and activation,²⁰ and TAN-derived cytokines CXCL1, CC chemokine ligand (CCL)3, and CCL5, whereas these cytokines increased in mice treated with MDZ+PK11195. Moreover, CCL2, CCL3, CCL21, and CXCL13, which are associated with chronic pain in the dorsal horn of the spinal cord and the peripheral nervous system,²¹ increased in mice treated with MDZ+PK11195 compared with MDZ alone.

Midazolam inhibited proliferation of PDAC cell lines

Proliferation of PDAC derived cell lines *in vitro* was inhibited in the presence of MDZ or PK11195 *in vitro* (Fig. 5a). To understand the anti-proliferative mechanism of MDZ, we determined the expression of cyclins and cyclin-dependent kinases (CDKs). Midazolam and PK11195 inhibited cyclin B1 concentrations in the murine PDAC cell lines (Fig. 5b and c; Supplementary Fig. 15). Expression of cyclin D1 and A2 was inhibited by MDZ and PK11195 in one PDAC cell line (147), but the effect was uncertain in other cell lines (146 and 244). Midazolam reduced expression of CDK1 and CDK4 in the three PDAC cell lines, whereas CDK2 expression was reduced by MDZ in a PDAC cell (244). Flow cytometer analysis revealed MDZ induced G2/M arrest in murine PDAC cell lines (146 and 147) (Supplementary Figs. 16–18), whereas G0/G1 arrest increased in one cell line (244). Midazolam induced early apoptotic cells slightly and late apoptotic/necrotic cells more significantly (Supplementary Fig. 19). Proliferation of pancreatic stellate cells (PSCs), which are sources of activated α -SMA⁺ CAFs, was inhibited by MDZ in a concentration-dependent manner *in vitro* (Fig. 5d).

Discussion

Genetically engineered mouse models, which maintain the innate immuno-inflammatory system, can model cancer more accurately than transplant models using immunodeficient mice.²² To investigate the effects of MDZ on not only PDAC cells but also stroma cells, including CAFs and immuno-inflammatory cells, we used the KPPC genetic model.¹³ Alteration of the tumor-stromal microenvironments are summarised in Fig. 6a

We demonstrated downregulation of cyclins/CDKs and cell-cycle arrest and sequential induction of cell death in PDAC by MDZ. Previous reports indicate that MDZ induces downregulation of cyclins D and A, resulting in G0/G1 arrest and apoptosis in non-PDAC cell lines.^{2,23} Induction of non-apoptotic cell death can result from p53-hetero-knockout in PDAC cell lines.¹⁴ Although recent studies indicate that MDZ modulates not only the cell cycle but also the mitochondrial caspase pathway, endoplasmic reticulum stress, and autophagy to induce apoptosis,²⁴ downregulation of cyclins/CDKs and the sequential cell-cycle arrest and induction of apoptotic and non-apoptotic cell death could be key mechanisms of MDZ in PDAC cells.

The inhibitory potential on proliferation by PK11195 may result as an agonist rather than antagonist of peripheral TSPO. PK11195 shows anti-proliferative and pro-apoptotic reactions in glioblastoma cell lines *in vitro* and *in vivo*.²⁵ We showed an

anti-proliferative potential of MDZ and PK11195 for PDAC and PSC lines *in vitro*. Pancreatic ductal adenocarcinoma cells and PSCs/CAFs secrete several cytokines and stimulate each other's proliferative potential.¹⁶ Nonetheless, the proliferation of PDAC increased in mice treated with MDZ+PK11195, indicating that increased proliferative potential by PK11195 does not result from PDAC- and CAF-mediated factors.

Tumour-associated inflammatory cells play an important role in the development and progression of PDAC.¹⁰ Previous reports showed that MDZ inhibits activation of neutrophils and macrophages in non-cancer lesions,⁹ whereas PK11195 antagonises these functions. Similarly, we observed MDZ-induced inhibition of local infiltration of TANs, M2-like TAMs, and PMN-MDSCs. It is difficult to distinguish anti-tumour N1 and tumour-promoting N2 TANs clearly by immunohistochemistry, but our results suggest that the function of N2 TANs might be inhibited by MDZ.¹¹ In addition, decreased soluble vascular cell adhesion molecule-1, intercellular adhesion molecule-1, and P-selectin, which are expressed on activated endothelium and related to leucocyte–endothelial interactions,^{26,27} might also reduce leucocyte migration from blood vessels to local lesions.

Inflammatory cytokines secreted from PDAC, CAFs,¹⁶ and inflammatory cells are involved in the mechanism of inflammatory pain.¹² Involvement of MDZ in inflammatory cells and the related cytokines are shown in Fig. 6b. We observed reduced inflammatory cytokines by MDZ, including IL-6. A recent study indicates that PSC/CAF-derived IL-6 promotes myeloid-derived suppressor cell differentiation and expansion from peripheral blood monocytes.²⁸ Myeloid-derived suppressor cells serve as a source of IL-6 in tumour-bearing mice,²⁹ whereas depletion of IL-6 in a KRAS-induced PDAC mouse model revealed a decrease in intra-tumour myeloid-derived suppressor cells.³⁰ Recruitment and expansion of myeloid-derived suppressor cells³¹ are mediated by many inflammatory factors, such as IL-6, IL-10, GM-CSF, G-CSF, CCL2, and CCL5.³² These cytokines were reduced in our pancreatic cancer model mice by MDZ. Increased CCL5 promotes inflammatory and nociceptive pain in bone cancer metastasis.³³ The CCL5/CCR5 axis of myeloid-derived suppressor cells plays an important role in their recruitment and activation.³⁴ Although the direct mechanism remains unclear, inhibition of local infiltration of myeloid-derived suppressor cells by MDZ could improve inflammatory pain via inhibition of IL-6 and CCL5 concentrations.

Daily intraperitoneal injection of PK11195 cannot be ruled out for the increase in pain signs. Indeed, an increase in plasma chemokines, such as CCL2, CCL3, CCL5, CCL21, CXCL1, and CXCL13, by PK11195 treatment might enhance inflammatory pain through the dorsal horn of the spinal cord and the peripheral nervous system.^{21,35,36}

It is important to study the effects of MDZ on long-term outcomes, such as recurrence and disease-free survival after perioperative interventions, but operations, including surgical resection of cancer, are never managed with MDZ only. It is a limitation to investigate the effect of MDZ alone, but our findings provide useful information for anaesthesiologists and patients with PDAC.

In summary, midazolam suppresses the proliferation of pancreatic ductal adenocarcinoma and cancer-associated fibroblasts and the local infiltration of tumour-associated neutrophils, M2-like tumour-associated macrophages, and polymorphonuclear myeloid-derived suppressor cells, thereby inhibiting pancreatic ductal adenocarcinoma progression.

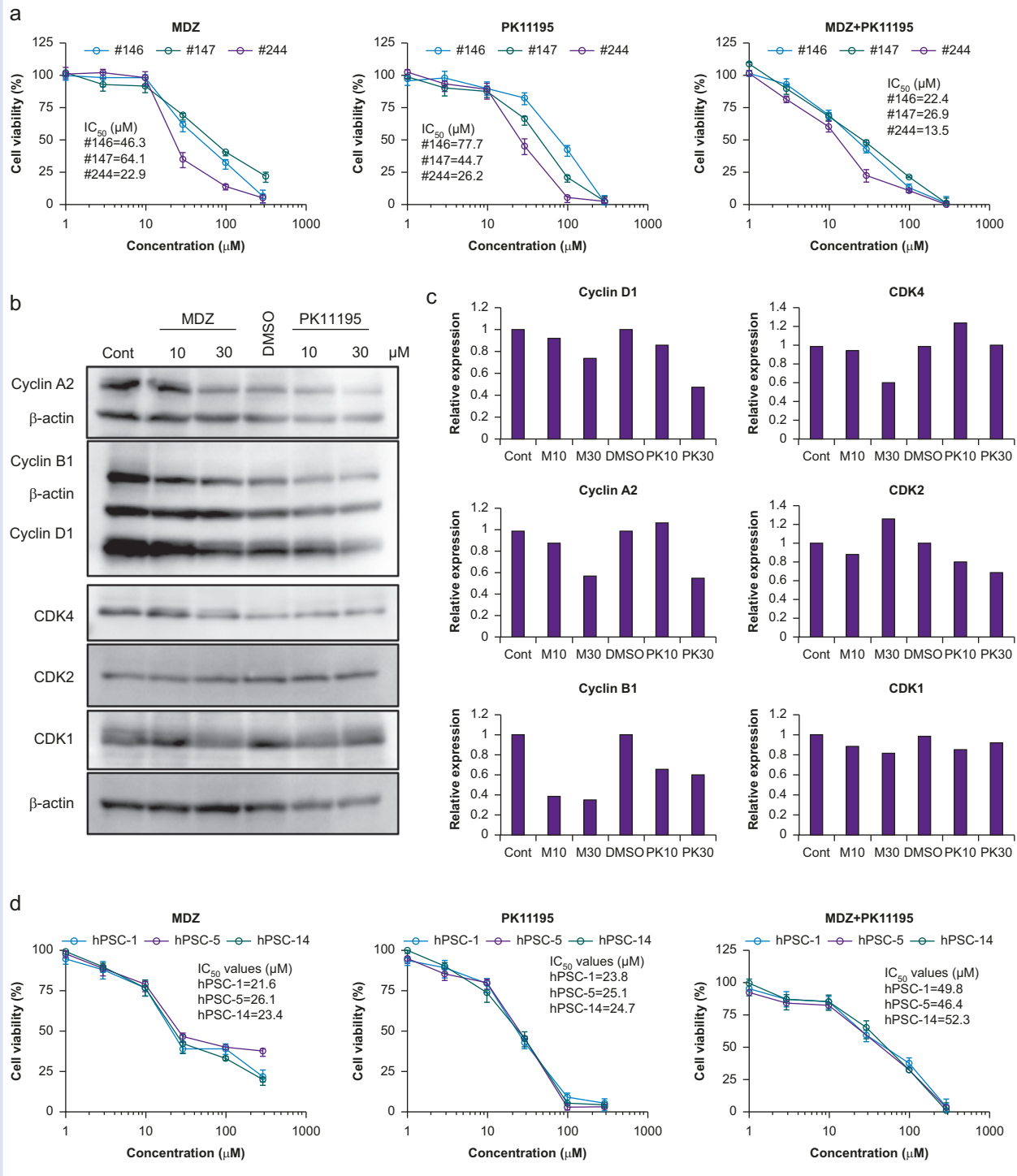
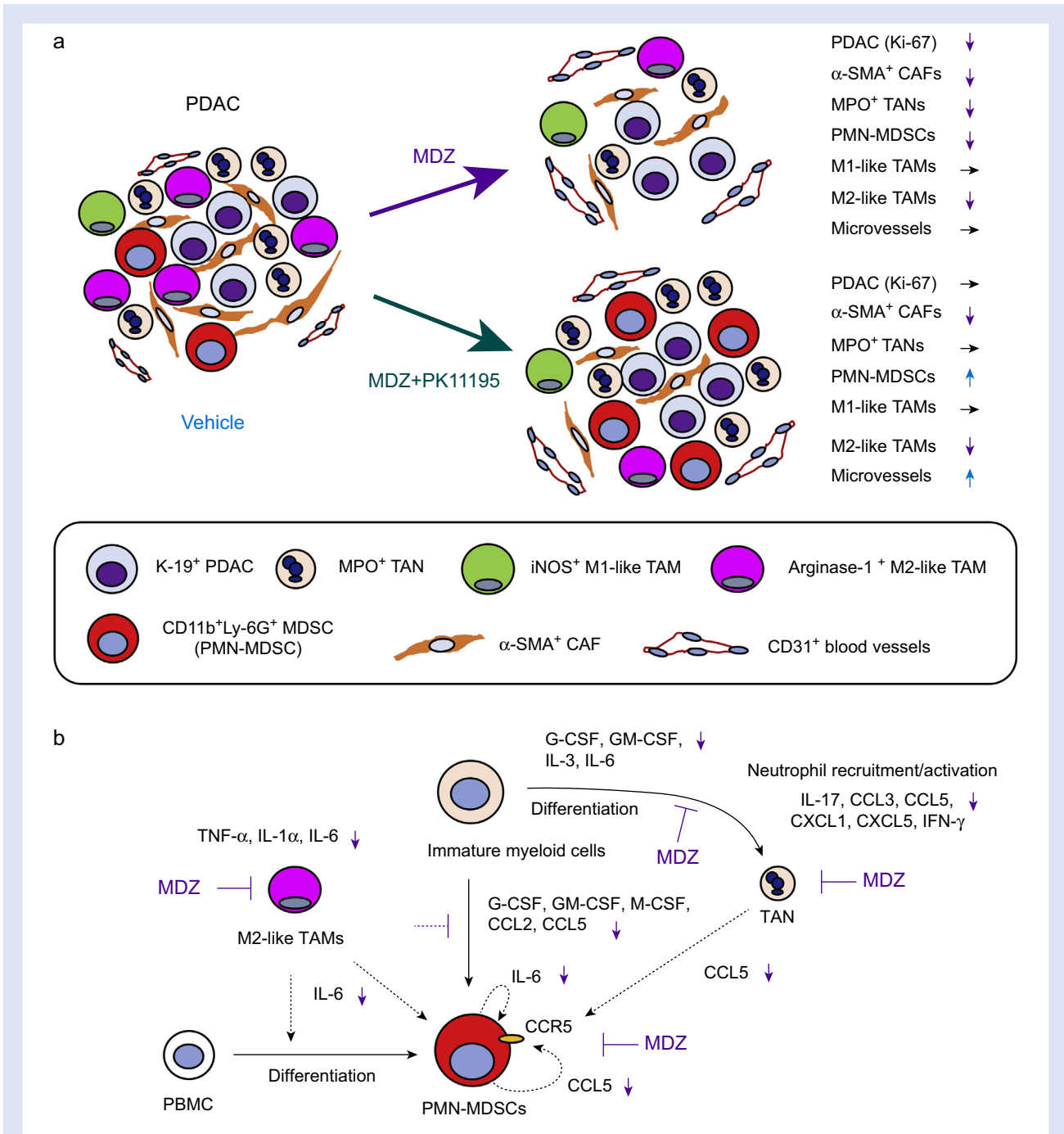


Fig 5. Anti-proliferative effects of midazolam in mouse PDAC and human pancreatic stellate cell lines. (a) Proliferation of mouse pancreatic ductal adenocarcinoma cell lines (#146, 147, and 244) was inhibited by MDZ and PK11195. Data are presented as mean (SD). (b) Immunoblotting of cyclins D1, A2, B1, CDK4, CDK2, and CDK1 in a pancreatic ductal adenocarcinoma cells (#147; Cont, water control for MDZ; DMSO control for PK). (c) Quantification of the data in (b). (d) Proliferation of human pancreatic stellate cells (hPSC-1, 5, and 14) was inhibited by MDZ and PK11195. Data are presented as mean (SD). CDK, cyclin-dependent kinase; DMSO, dimethyl sulphoxide; hPSC, human pancreatic stellate cell; MDZ, midazolam; PDAC, pancreatic ductal adenocarcinoma.



Authors' contributions

Experiment design: MS, TS
 Data acquisition/analysis: MS, YO
 Provision of vehicle-treated KPCC data: IK
 Proliferative analysis: YIC
 Analysis of induction of apoptosis by flow cytometry: EH
 Tissue preparation/staining: JK
 Pathological confirmation of pancreatic tumours: YM
 Provision of human pancreatic stellate cells: AM
 Discussion of data: TI, TK, OK, YIs
 Writing of paper: MS, YO
 Review of paper: HI, TS
 Study supervision: TS

Acknowledgements

The authors thank members of the Animal Laboratory for assisting with animal care, and Enago (www.enago.jp) for English language review.

Declarations of interest

The authors declare that they have no conflicts of interest.

Funding

Japan Society for the Promotion of Science KAKENHI (JP21K09006).

Appendix A. Supplementary data

Supplementary data to this article can be found online at <https://doi.org/10.1016/j.bja.2021.12.042>.

References

- Snyder GL, Greenberg S. Effect of anaesthetic technique and other perioperative factors on cancer recurrence. *Br J Anaesth* 2010; **105**: 106–15
- Wang C, Dattoo T, Zhao H, et al. Midazolam and dexmedetomidine affect neuroglioma and lung carcinoma cell biology in vitro and in vivo. *Anesthesiology* 2018; **129**: 1000–14
- Lavon H, Matzner P, Benbenishty A, et al. Dexmedetomidine promotes metastasis in rodent models of breast, lung, and colon cancers. *Br J Anaesth* 2018; **120**: 188–96
- Adams R, Brown GT, Davidson M, et al. Efficacy of dexmedetomidine compared with midazolam for sedation in adult intensive care patients: a systematic review. *Br J Anaesth* 2013; **111**: 703–10
- Prommer E. Midazolam: an essential palliative care drug. *Palliat Care Soc Pract* 2020; **14**: 2632352419895527
- Bhoola NH, Mbita Z, Hull R, Dlamini Z. Translocator protein (TSPO) as a potential biomarker in human cancers. *Int J Mol Sci* 2018; **19**: 2176
- Cohen AS, Li J, Hight MR, et al. TSPO-targeted PET and optical probes for the detection and localization of pre-malignant and malignant pancreatic lesions. *Clin Cancer Res* 2020; **26**: 5914–25
- Siegel RL, Miller KD, Jemal A. Cancer statistics, 2020. *CA Cancer J Clin* 2020; **70**: 7–30
- Cruz FF, Rocco PR, Pelosi P. Anti-inflammatory properties of anesthetic agents. *Crit Care* 2017; **21**: 67
- Huber M, Brehm CU, Gress TM, et al. The immune microenvironment in pancreatic cancer. *Int J Mol Sci* 2020; **21**: 7307
- Keeley T, Costanzo-Garvey DL, Cook LM. Unmasking the many faces of tumor-associated neutrophils and macrophages: considerations for targeting innate immune cells in cancer. *Trends Cancer* 2019; **5**: 789–98
- Fitzgibbon DR, Loese JD. *Cancer pain: assessment, diagnosis, and management*. 1st Edn. Philadelphia, PA: Lippincott Williams & Wilkins/Wolters Kluwer Health; 2010
- Kajiwara I, Sano M, Ichimaru Y, et al. Duloxetine improves cancer-associated pain in a mouse model of pancreatic cancer through stimulation of noradrenaline pathway and its antitumor effects. *Pain* 2020; **161**: 2909–19
- Ichimaru Y, Sano M, Kajiwara I, et al. Indirubin 3'-oxime inhibits migration, invasion, and metastasis in vivo in mice bearing spontaneously occurring pancreatic cancer via blocking the RAF/ERK, AKT, and SAPK/JNK pathways. *Transl Oncol* 2019; **12**: 1574–82
- Sano M, Ichimaru Y, Kurita M, et al. Induction of cell death in pancreatic ductal adenocarcinoma by indirubin 3'-oxime and 5-methoxyindirubin 3'-oxime in vitro and in vivo. *Cancer Lett* 2017; **397**: 72–82
- Sano M, Ijichi H, Takahashi R, et al. Blocking CXCLs-CXCR2 axis in tumor-stromal interactions contributes to survival in a mouse model of pancreatic ductal adenocarcinoma through reduced cell invasion/migration and a shift of immune-inflammatory microenvironment. *Oncogenesis* 2019; **8**: 8
- Sano M, Takahashi R, Ijichi H, et al. Blocking VCAM-1 inhibits pancreatic tumour progression and cancer-associated thrombosis/thromboembolism. *Gut* 2021; **70**: 1713–23
- Kanda Y. Investigation of the freely available easy-to-use software 'EZ' for medical statistics. *Bone Marrow Transplant* 2013; **48**: 452–8
- Gabitass RF, Annels NE, Stocken DD, Pandha HA, Middleton GW. Elevated myeloid-derived suppressor cells in pancreatic, esophageal and gastric cancer are an independent prognostic factor and are associated with significant elevation of the Th2 cytokine interleukin-13. *Cancer Immunol Immunother* 2011; **60**: 1419–30
- Sionov RV, Fridlender ZG, Granot Z. The multifaceted roles neutrophils play in the tumor microenvironment. *Cancer Microenviron* 2015; **8**: 125–58
- Montague K, Malcangio M. The therapeutic potential of targeting chemokine signalling in the treatment of chronic pain. *J Neurochem* 2017; **141**: 520–31
- Zitvogel L, Pitt JM, Daille R, Smyth MJ, Kroemer G. Mouse models in oncoimmunology. *Nat Rev Cancer* 2016; **16**: 759–73
- Qi Y, Yao X, Du X. Midazolam inhibits proliferation and accelerates apoptosis of hepatocellular carcinoma cells by elevating microRNA-124-3p and suppressing PIM-1. *IUBMB Life* 2020; **72**: 452–64
- So EC, Chen YC, Wang SC, et al. Midazolam regulated caspase pathway, endoplasmic reticulum stress, autophagy, and cell cycle to induce apoptosis in MA-10 mouse Leydig tumor cells. *Oncotargets Ther* 2016; **9**: 2519–33
- Ammer LM, Vollmann-Zwerenz A, Ruf V, et al. The role of translocator protein TSPO in hallmarks of glioblastoma. *Cancers (Basel)* 2020; **12**: 2973

26. Joo HK, Oh SC, Cho EJ, et al. Midazolam inhibits tumor necrosis factor- α -induced endothelial activation: involvement of the peripheral benzodiazepine receptor. *Anesthesiology* 2009; **110**: 106–12
27. Ghori K, Harmon D, Lan W, Seigne P, Walsh F, Shorten GD. The effect of midazolam on cerebral endothelial (P-selectin and ICAM-1) adhesion molecule expression during hypoxia-reperfusion injury in vitro. *Eur J Anaesthesiol* 2008; **25**: 206–10
28. Mace TA, Ameen Z, Collins A, et al. Pancreatic cancer-associated stellate cells promote differentiation of myeloid-derived suppressor cells in a STAT3-dependent manner. *Cancer Res* 2013; **73**: 3007–18
29. Tsukamoto H, Nishikata R, Senju S, Nishimura Y. Myeloid-derived suppressor cells attenuate TH1 development through IL-6 production to promote tumor progression. *Cancer Immunol Res* 2013; **1**: 64–76
30. Zhang Y, Yan W, Collins MA, et al. Interleukin-6 is required for pancreatic cancer progression by promoting MAPK signaling activation and oxidative stress resistance. *Cancer Res* 2013; **73**: 6359–74
31. Bronte V, Brandau S, Chen SH, et al. Recommendations for myeloid-derived suppressor cell nomenclature and characterization standards. *Nat Commun* 2016; **7**: 12150
32. Groth C, Hu X, Weber R, et al. Immunosuppression mediated by myeloid-derived suppressor cells (MDSCs) during tumour progression. *Br J Cancer* 2019; **120**: 16–25
33. Di Pompo G, Lemma S, Canti L, et al. Intratumoral acidosis fosters cancer-induced bone pain through the activation of the mesenchymal tumor-associated stroma in bone metastasis from breast carcinoma. *Oncotarget* 2017; **8**: 54478–96
34. Blattner C, Fleming V, Weber R, et al. CCR5⁺ myeloid-derived suppressor cells are enriched and activated in melanoma lesions. *Cancer Res* 2018; **78**: 157–67
35. Cao DL, Zhang ZJ, Xie RG, Jiang BC, Ji RR, Gao YJ. Chemokine CXCL1 enhances inflammatory pain and increases NMDA receptor activity and COX-2 expression in spinal cord neurons via activation of CXCR2. *Exp Neurol* 2014; **261**: 328–36
36. Hang LH, Shao DH, Chen Z, Chen YF, Shu WW, Zhao ZG. Involvement of spinal CC chemokine ligand 5 in the development of bone cancer pain in rats. *Basic Clin Pharmacol Toxicol* 2013; **113**: 325–8

Handling editor: Hugh C Hemmings Jr

主論文の和文の要約

ミダゾラムの膵癌自然発症マウスにおける抗腫瘍・抗炎症効果と癌性疼痛の改善効果

外科系麻酔科学専攻 大島雪乃

【背景】近年、手術中の麻酔・周術期管理が患者の長期予後に影響することが報告され、鎮痛・鎮静薬のなかには細胞性免疫を抑制することが知られているが、膵癌におけるミダゾラムの効果は未だに不明である。今回、ミダゾラムの膵癌に対する抗腫瘍・抗炎症効果ならびに癌性疼痛への影響を明らかにするため、膵癌の自然発症モデルである KPPC マウス (LSL-KrasG12D/+;Trp53flox/flox;Pdx-1cre/+マウス) を用いて検討を行った。

【方法】遺伝子組換え委員会と動物実験委員会の承認を得た後、6週齢の KPPC マウスを3群に分け、① 30 mg/kg/day のミダゾラム (MDZ) 投与群 (n=13)、② 30 mg/kg/day の MDZ と 3 mg/kg/day の末梢性ベンゾジアゼピン受容体拮抗薬である PK11195 (PK) の MDZ+PK 投与群 (n=10)、③ 飲水のみのコントロール群(n=14)とした。生存曲線を Kaplan-Meier 法により求め、統計学的に Log-rank 検定を行った。癌性疼痛は Hunching と mouse grimace scale (MGS) でスコアリングし、one-way ANOVA 後の Tukey 検定を行った。エンドポイント時には膵腫瘍と全身諸臓器をサンプリングし、免疫組織化学的解析を行い、Tukey-Kramer 検定もしくは Steel-Dwass 検定を行った。各検定の $p < 0.05$ で有意差ありとした。血漿サイトカインの動態をサイトカイン抗体アレイにより半網羅的に解析した。MDZ の膵癌細胞株の増殖への影響を AlamarBlue 法にて検討し、細胞周期関連分子の発現をウェスタンブロッティング、アポトーシスの誘導に関してはフローサイトメーターにて解析した。

【結果ならびに考察】MDZ 群の膵管癌においては細胞増殖に関わる Ki-67, サイクリン D1, A2, B1 の陽性率はコントロール群と比較して有意に低下し、腫瘍体積が有意に縮小した。生存期間では有意差が得られなかった。また、MDZ 群では癌関連線維芽細胞 (CAF) の増殖を抑制し、腫瘍関連好中球 (TAN) や M2 様腫瘍関連マクロファージ (TAM), 多形核骨髄由来免疫抑制細胞 (PMN-MDSC) の局所浸潤を抑制した。一方、MDZ+PK 群においては CAF の増殖と M2 様 TAM の浸潤は抑制されたが、TAN と PMN-MDSC の浸潤は MDZ 群と比較して増加した。疼痛評価においても MDZ 群で Hunching と MGS スコアの低下を認めたのに対し、MDZ+PK 群ではコントロール群よりも両スコアが増加した。MDZ 群の血漿 $TNF\alpha$, $IL-1\alpha$, $IL-6$, $CCL2$, $CCL3$, $CCL5$, $CXCL1$ はコントロール群と比較して減少し、MDZ+PK 群で $TNF\alpha$ を除くサイトカインの増加を認めた。In vitro 解析においては MDZ が膵癌細胞株のサイクリンや CDK を低下させ、増殖を抑制し、後期アポトーシスを誘導した。これらの結果から、MDZ は膵癌マウスモデルにおいて膵癌細胞と CAF の増殖を抑制し、さらに TAN や M2 様 TAM, PMN-MDSC の局所浸潤を抑制することで炎症性サイトカインを低下させ、炎症性疼痛の軽減に寄与したことが考えられた。

【結語】MDZ は膵癌に対して抗腫瘍・抗炎症効果ならびに疼痛緩和効果を示す。